Space Sci Rev (2010) 151: 25–38
DOI 10.1007/s11214-009-9591-9

MICROSCOPE On-ground and In-orbit Calibration

Vincent Josselin · Pierre Touboul · Manuel Rodrigues · Françoise Liorzou

Received: 23 December 2008 / Accepted: 2 November 2009 / Published online: 18 March 2010

Abstract The MICROSCOPE mission, to be launched in 2011, will perform the test of the universality of free fall (Equivalence Principle) to an accuracy of 10^{-15}. The payload consists of two sensors, each controlling the free fall of a pair of test masses: the first for the test of the Equivalence Principle (titanium/platinum), the second for performance verification (platinum/platinum).

The capability to detect a faint violation signal of the EP test is conditioned upon the rejection of disturbances arising from the coupling and misalignments of the instrument vectorial outputs. Therefore the performance of the mission depends on the success of the series of calibration operations which are planned during the satellite life in orbit. These operations involve forced motion of the masses with respect to the satellite.

Specific data processing tools and simulations are integral parts of the calibration and performance enhancement process, as are the tests operated on ground at the ZARM drop tower. The presentation will focus on the current status of the MICROSCOPE payload, the rationale for the in-orbit calibrations, the data processing operations and the tests performed at the ZARM drop tower.

Keywords Equivalence principle · Gravity · MICROSCOPE · Calibration · Accelerometer

1 Introduction: Overview of the MICROSCOPE Mission

1.1 The MICROSCOPE Mission

The MICROSCOPE mission is dedicated to the test of the Equivalence Principle (EP) to an accuracy of 10^{-15} (Touboul and Rodrigues 2001). The satellite is part of the MYRIAD family of micro-satellite developed by the Centre National d'Études Spatiales (CNES): the satellite weighs less than 200 kg with a payload of about 40 kg, 50 dm^3, and 40 W. ONERA, the French Aerospace Labs is in charge of the scientific payload development and data

V. Josselin (✉) · P. Touboul · M. Rodrigues · F. Liorzou
ONERA, BP72-29 avenue de la Division Leclerc, 92322 Chatillon Cedex, France
e-mail: vincent.josselin@onera.fr

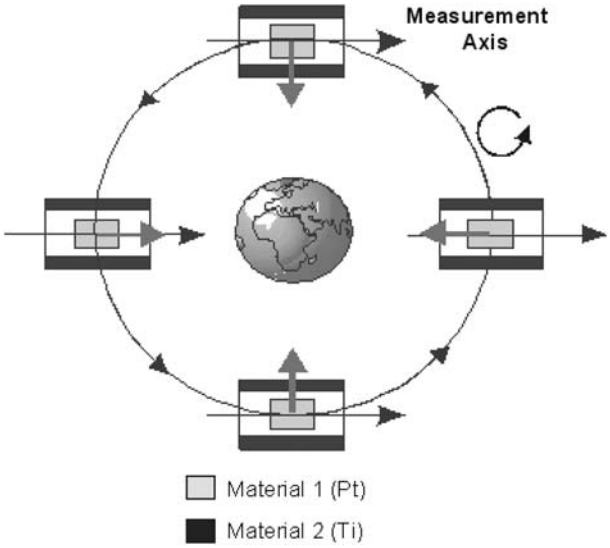

Fig. 1 MICROSCOPE experiment concept: the two masses fall around the Earth, controlled along the same orbit, either in inertial pointing (*straight black arrows*) or spinning around the normal to the orbit (*curled black arrow*). In case of EP violation, the difference of electrostatic forces actuated by the servo-control to maintain the masses motionless (*grey arrows*) is accurately measured

processing with support from the Observatoire de la Côte d'Azur (OCA) and from the Bremen University (ZARM). The MICROSCOPE satellite launch is scheduled in 2011. It will fly at an altitude of 810 km along a quasi-polar and heliosynchronous orbit with a 5×10^{-3} eccentricity. This low eclipse rate orbit will result in a very stable thermal environment for the payload.

The MICROSCOPE mission is part of the current effort in fundamental physics to focus on the research of new interactions or of a slightly modified gravitational potential. The test of the Equivalence Principle, which states that inertial and gravitational masses are equivalent, is a key point: an improvement in the confirmation of the equivalence between inertial mass and gravitational mass represents an important verification of the relativistic gravitation and other metric theories which postulate this principle, and it emphasizes the interest of more accurate experimentation for the determination of Post-Newtonian coefficients. A violation of the Equivalence Principle, which is the exact symmetry required for General Relativity, would certainly lead to evidence of a new interaction that is predicted by many quantum theories of gravity. A new massless scalar field that causes the EP violation could be detected by EP test experimentation, which is one of the most sensitive low energy probes.

The most accurate experiments to date use torsion pendulums in ground based laboratories, and they have to deal with environmental instabilities induced in particular by Earth gravity gradient fluctuations and human activities. Important results have also been obtained by the accurate laser ranging of the Earth–Moon relative motion in the Sun gravity field: in addition to the ranging accuracy, the material composition of the two celestial bodies is a limitation for the interpretation of the results.

In the MICROSCOPE experiment, the Earth is the gravitational source about which free-fall motion of two masses, composed of different materials, is observed and controlled taking care that both masses are submitted exactly to the same gravitational field as sketched in Fig. 1. The controlled electrostatic actuation forces the masses to remain on the same orbit which is accurately measured: a defect of the actuation symmetry gives rise to evidence of an EP violation.

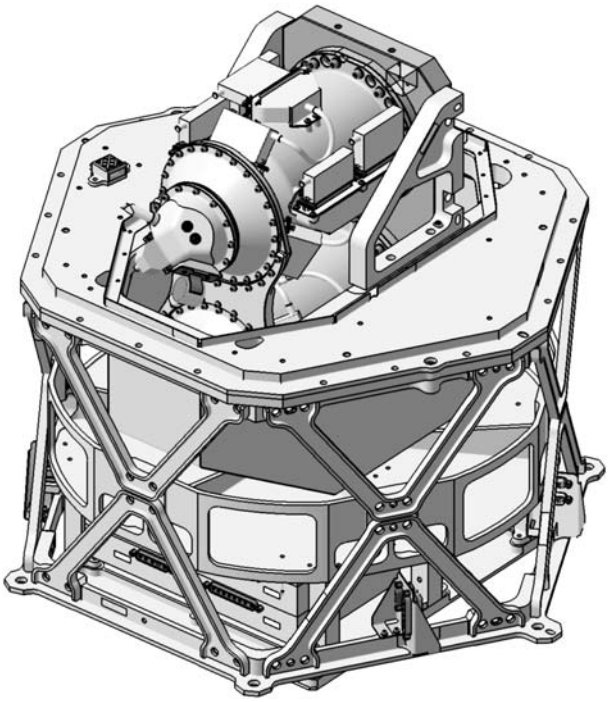

Fig. 2 Accommodation of the payload on the MICROSCOPE Satellite. Important care has been paid to the thermal and magnetic environment stability

This space experiment exploits the very soft accelerometric environment delivered on board by a dedicated compact satellite including a drag compensation system: the surface forces applied on the satellite are counteracted continuously by the thrust of the electrical propulsion system. The observation period of the mass motions in free fall in steady conditions leads to expected signal integration over days and weeks and thus to a high rejection of stochastic disturbances. Rotations of the observational frame with respect to the Earth's gravity field frame help also in the discrimination of the eventual EP violation signal from the instrument and environment sources of noise. Several rotation frequencies are considered around 10^{-3} Hz with well selected phases with respect to the satellite position on its orbit: frequency analyses with heterodyne detection are then considered in the data processing.

1.2 The MICROSCOPE Payload

The MICROSCOPE payload consists of two independent "Space Accelerometer for Gravity Experiment" (SAGE) instruments: the first designed for the EP test with platinum/titanium masses and the second one for verification as reference with platinum/platinum masses. The sensors operation is based on the principle of a digital servo-control of the motion of the test masses with capacitive position sensing and electrostatic actuation. The SAGE instrument consists of 3 units:

- The "Sensor Unit" (SU) comprises two quasi cylindrical and co-axial test masses and two silica cores surrounding these masses, both being included in the same instrument tight housing (see Fig. 3, right),
- The "Front-End Electronic Unit" (FEEU) handles the low-noise analog functions: capacitive sensing of both masses, reference voltage sources and amplification of the control voltage for the electrostatic actuation,

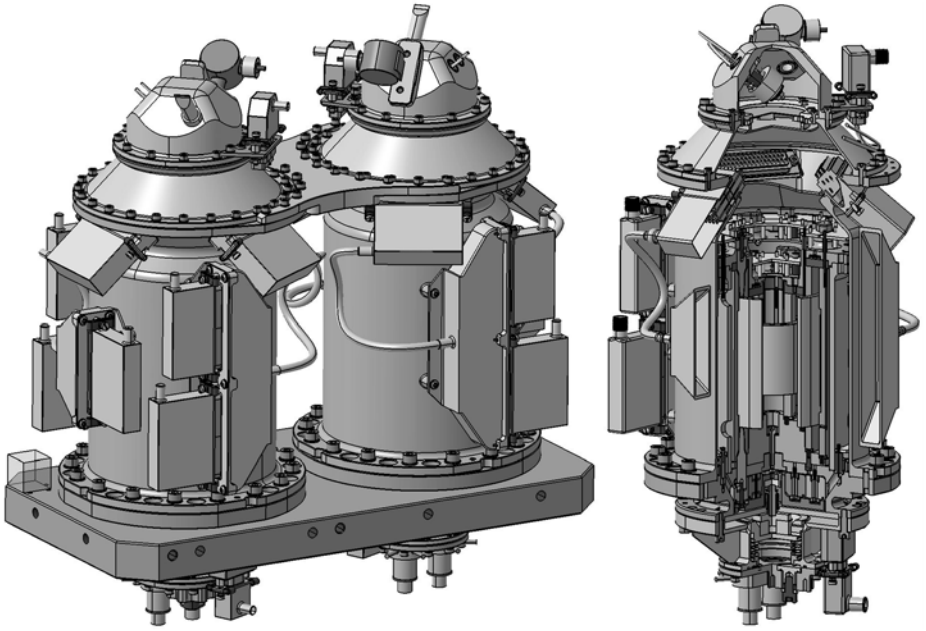

Fig. 3 Mechanical core. *Left*, sketch of the two SU sensors, REFerence (platinum/platinum) and EP (platinum/titanium). *Right*, sensor core of the differential accelerometer including a tight housing with its ionic pump and getter, its ring of connectors, four cylindrical glass ceramic electrode supports, two concentric masses and one blocking mechanism (*from right to left*)

– The "Interface Control Unit" (ICU) hosts the digital electronics for the servo-control of the servo-loops and the interfaces to the data bus of the satellite. The ICU includes also the power converters. For practical reasons of accommodation, the two payload ICUs are stacked and form the "Interface and Control Unit Mechanical Ensemble" (ICUME).

The satellite payload is operated in a finely stabilised temperature environment and protected from perturbations by a magnetic shield (see Fig. 2). The two differential accelerometers are mounted on a common soleplate as sketched in Fig. 3 (left). The T-SAGE instrument can be operated in:

– Stand-by Mode (SBY); the mass motion is not sensed, the servo-control delivers no actuation;
– Position Sensing Mode (PSM); the mass motion is sensed (providing 3 position outputs and 3 attitude outputs) and available as telemetry, the servo-control delivers no actuation;
– Acceleration Sensing Mode (ASM); the 6-channel servo-control is fully operating, either in the full-range (FR) or in high-resolution configuration (HR). Telemetry is available with the mass displacements and accelerations along all degrees of freedom.

The full-range configuration is devoted to the levitation of the test masses thanks to stiffer and more robust control laws whereas the high-resolution configuration is optimised for delivering the scientific data at the ultimate resolution.

The full-range configuration is also a back-up option when residual vibrations or drag forces are too high for the high-resolution servo-control to withstand them. Before the first in-orbit switch on (and so during the launch), the test mass of each inertial sensor is clamped

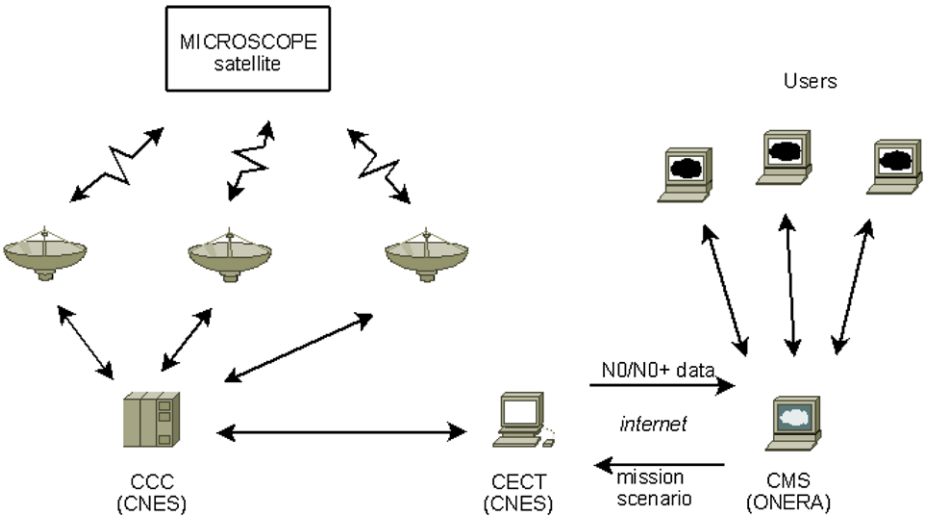

Fig. 4 Sketch of the MICROSCOPE "Centre de Mission Scientifique" (CMS): interfaces with the "Centre d'Expertise et de Contrôle de Trainéee" (CECT) and interface with the users

by the Test-Mass Blocking Mechanism. In this configuration, the sensors can sustain the launch accelerations and vibrations.

1.3 MICROSCOPE Ground Segment for Data Processing

The mission science centre, CMS ("Centre de Mission Scientifique" in French), will be located at the Châtillon premises of ONERA. Its tasks include:

- Download the telemetry data from the CNES control ground segment, 'Centre d'Expertise et de Contrôle de Trainée' (CECT);
- Prepare telecommand packets to be sent to the satellite via the CECT for payload and platform operational modifications (calibrations, measurements, . . .);
- Perform maintenance task of data verification and archiving;
- Set up a client/server platform for operating the data processing linked to the EP test;
- Set up a HTTP server for the supervision of the payload;
- Set up a FTP server for data distribution to the other authorised scientific centres.

Figure 4 provides a sketch of the CMS interfaces with CECT and users. The CMS handles different levels of data:

- Raw Data: telemetry data coming from the satellite.
- Level 0 Data (N0): obtained through re-formatting of the raw data and by adding complementary information from other systems.
- Level 1 Data (N1): obtained from N0 data after pre-processing with a priori known characteristics of the instrumental parameters. These data shall also be corrected by taking advantage of the in-orbit calibration phases. They mainly concern the inertial sensor data.
- Level 2 Data (N2): derived from level 1 calibrated data. They mainly concern the differential data comparing the accelerations of two test masses. They benefit from all a priori and a posteriori knowledge of the instrument operation and environment, of the space experiment procedures and of the scientific data processing and analyses.

2 In-orbit Instrument Calibration

2.1 EP Measurement and Performance Assessment

The mission shall provide a test of the Equivalence Principle with an accuracy of 10^{-15}. Each single test measure shall have this accuracy with a signal to noise ratio of at least one. The accuracy of the result is improved by the permanent survey of the instrument operation, calibration and environment. The accuracy is also improved by the number of measurement sequences in different experimental conditions. The two differential accelerometers composing the payload provide the scientific signals that will be associated to the star-sensor outputs, to the drag-free and attitude control system housekeeping data, to the thermal environment survey and to the orbit a posteriori determination. The six acceleration signals (one per degree of freedom) from the control of each of the test masses will be particularly analysed at the specific frequency f_{EP}, corresponding to the modulation frequency of the Earth gravity field along the instrument axes, where the EP test is performed.

The EP test consists simply in processing the difference of acceleration Γ_d measured by the two concentric inertial sensors made of different materials. It may involve subtracting disturbances measured by the second differential accelerometer made of the same materials.

The total force applied on the test mass k is composed of

- Electrostatic forces applied by electrodes, $\overrightarrow{F_{el_k}}$,
- Gravitational force in the Earth field, $\int_{P\in\mathrm{mass}} \overrightarrow{g(P)}\, dm_{Gk}$,
- Parasitic forces, $\overrightarrow{F_{pa_k}}$,

resulting in the equation of the test-mass acceleration:

$$m_{Ik}\overrightarrow{\gamma(O_k)} = \overrightarrow{F_{el_k}} + \int_{P\in\mathrm{mass}} \overrightarrow{g(P)}\, dm_{Gk} + \overrightarrow{F_{pa_k}}, \tag{1}$$

where m_{Ik} is the inertial mass, with centre of mass O_k defined as

$$\int_{P\in\mathrm{mass}} \overrightarrow{O_kP}\, dm_{Ik} = \overrightarrow{0} \tag{2}$$

and where m_{Gk} is the gravitational mass, with centre of gravity G_k defined as

$$\int_{P\in\mathrm{mass}} \overrightarrow{G_kP} \wedge \overrightarrow{g\,(P)}\, dm_{Gk} = \overrightarrow{0}\,. \tag{3}$$

The test-mass acceleration is not directly measured but derived from measurement of the actuation force applied on the mass by the servo-control to maintain it at the centre of the sensor core. The electrostatic force is, minus biases and other spurious effects, proportional to the potential applied on the electrodes. Considering that the centre of gravity is close enough to the centre of inertia of the test mass, the measurement equation is then

$$\hat{\overrightarrow{\Gamma_{\mathrm{EP}}}} = \overrightarrow{\Gamma_{\mathrm{app},k}} = \frac{\overrightarrow{F_{el_k}}}{m_{Ik}} = \overrightarrow{\gamma\,(O_k)} - \frac{m_{Gk}}{m_{Ik}}\overrightarrow{g\,(O_k)} - \frac{\overrightarrow{F_{pa_k}}}{m_{Ik}} + O\left(2\times 10^{-17}\ \mathrm{m/s^2}\right). \tag{4}$$

The parameter δ_k from

$$\frac{m_{Gk}}{m_{Ik}} = 1 + \delta_k \tag{5}$$

is non-null if the equivalence principle is violated within the accuracy reach of the MICROSCOPE mission. It is identical at first order to the von Oëtvos parameter. The acceleration $\overrightarrow{\hat{\Gamma}_{\mathrm{EP}}}$ is measured in the satellite reference frame in which the instrument structure carrying the electrostatic actuators are mounted. Considering the attitude motion of the satellite, we get for each mass:

$$\begin{aligned}\overrightarrow{\Gamma_{\mathrm{app},k}} = \overrightarrow{\gamma(O_{\mathrm{sat}})} + \dot{\overrightarrow{\Omega}} \wedge \overrightarrow{O_{\mathrm{sat}}O_k} + \overrightarrow{\Omega} \wedge \left(\overrightarrow{\Omega} \wedge \overrightarrow{O_{\mathrm{sat}}O_k}\right) + 2\overrightarrow{\Omega} \wedge \dot{\overrightarrow{O_{\mathrm{sat}}O_k}} + \ddot{\overrightarrow{O_{\mathrm{sat}}O_k}} \\ - (1+\delta_k)\overrightarrow{g(O_k)} - \frac{\overrightarrow{F_{pa_k}}}{m_{Ik}}. \end{aligned} \tag{6}$$

The differential signal from the differential accelerometer gathers the possible violation signal, driven by the $\delta = \delta_2 - \delta_1$ coefficient:

$$\begin{aligned}\overrightarrow{\Gamma_{\mathrm{app},d}} = \frac{\delta_2 - \delta_1}{2} \cdot \begin{pmatrix} g_x \\ g_y \\ g_z \end{pmatrix} + \frac{1}{2} \cdot \left[\begin{pmatrix} T_{xx} & T_{xy} & T_{xz} \\ T_{yx} & T_{yy} & T_{yz} \\ T_{zx} & T_{zy} & T_{zz} \end{pmatrix}_{|\mathrm{sat}} \right. \\ \left. - \begin{pmatrix} \mathrm{In}_{xx} & \mathrm{In}_{xy} & \mathrm{In}_{xz} \\ \mathrm{In}_{yx} & \mathrm{In}_{yy} & \mathrm{In}_{yz} \\ \mathrm{In}_{zx} & \mathrm{In}_{zy} & \mathrm{In}_{zz} \end{pmatrix}_{|\mathrm{sat}} \right] \cdot \begin{pmatrix} \Delta_x \\ \Delta_y \\ \Delta_z \end{pmatrix}_{|\mathrm{sat}} \end{aligned} \tag{7}$$

with

- $\overrightarrow{\Gamma_{\mathrm{app},d}}$, the difference of the measured acceleration by sensor 1 and 2,
- $[\mathsf{In}]$, the inertial tensor verifying: $[\mathsf{In}]\overrightarrow{O_{\mathrm{sat}}O_k} = \dot{\overrightarrow{\Omega}} \wedge \overrightarrow{O_{\mathrm{sat}}O_k} + \overrightarrow{\Omega} \wedge (\overrightarrow{\Omega} \wedge \overrightarrow{O_{\mathrm{sat}}O_k})$,
- $[\mathsf{T}]$, the gravitational tensor verifying at the first order: $[\mathsf{T}]\overrightarrow{O_iO_j} = \overrightarrow{g(O_j)} - \overrightarrow{g(O_i)}$,
- $\overrightarrow{\Delta}$, the relative mis-centring of the test masses.

The previous equations correspond to perfect sensors. Physical limitations are introduced:

- $\overrightarrow{b_{0k}}$ the sensor bias,
- $[\mathsf{M}_k]$ the sensitivity matrix combining the scale factor defects $[1 + \mathsf{dK}_{1k}]$ and the intra-axes coupling $[\eta_k]$,
- $[\Theta_k]$ the matrix modelling the alignment of the sensor with respect to the satellite reference frame,
- $\overrightarrow{F_{\mathrm{ext}}}$ the external force applied on the satellite surface,
- $\overrightarrow{F_{\mathrm{th}}}$ the thruster force applied by the satellite attitude and orbit control,
- $[\mathsf{K}_{2k}]$ the quadratic matrix,

leading to an acceleration measurement differing from the actual test-mass acceleration:

$$\begin{aligned}\overrightarrow{\Gamma_{\mathrm{meas},k}} = \overrightarrow{b_{0k}} + [\mathsf{M}_k] \cdot [\Theta_k] \cdot \left(\overrightarrow{\Gamma_{\mathrm{app},k}} + \frac{\overrightarrow{F_{\mathrm{ext}}}}{M_{\mathrm{sat}}} + \frac{\overrightarrow{F_{\mathrm{th}}}}{M_{\mathrm{sat}}} \right) \\ + [\mathsf{M}_k] \cdot \left(-\frac{\overrightarrow{F_{\mathrm{pa}}}}{m_{Ik}} - \frac{\overrightarrow{F_{\mathrm{el}}}}{m_{Ik}} \right) + [\mathsf{K}_{2k}] \cdot |\Gamma_{\mathrm{app},k}|^2 \frac{\overrightarrow{\Gamma_{\mathrm{app},k}}}{|\Gamma_{\mathrm{app},k}|}. \end{aligned} \tag{8}$$

2.2 Calibration Sequences

The MICROSCOPE mission relies on the calibration sequences to assess the disturbing parameters of Equation 8. It is an iterative process that takes advantage of both the capability

Table 1 Improvement of the knowledge of the parameters to be calibrated after one single round of calibration

Parameter to be calibrated	Specification	Performance after calibration
$K_{cx}\delta_x$	0.1 µm	0.14 µm
$K_{cx}\delta_z$	0.1 µm	0.14 µm
$K_{cx}\delta_y$	2 µm	6.9 µm
$(\eta_{cz}+\theta_{cz})$	0.9×10^{-3} rad	1.1×10^{-3} rad
$(\eta_{cy}-\theta_{cy})$	0.9×10^{-3} rad	1.1×10^{-3} rad
K_{dx}/K_{cx}	1.5×10^{-4}	5.7×10^{-4}
$\frac{\eta_{dz}+\theta_{dz}}{K_{cy}}$	5×10^{-5} rad	1.2×10^{-6} rad
$\frac{\eta_{dy}-\theta_{dy}}{K_{cz}}$	5×10^{-5} rad	1.2×10^{-6} rad
K_{2cxx}/K_{cx}^2	800 s^2/m	416 s^2/m
K_{2dxx}/K_{cx}^2	N/A	54 s^2/m

of the satellite orbit and attitude control system to force the motion of the satellite through its thrusters and the sensor servo-control to force the motion of the test masses (Guiu 2007). The fine assessment of the physical value of the parameters listed below are critical for allowing an efficient post-processing of the acceleration data of the SAGE instruments. There are ten parameters to calibrate, defined as follows:

- $K_{cx}\Delta_x$ by using the Earth's gravity gradient as signal,
- $K_{cx}\Delta_z$ by using the Earth's gravity gradient as signal,
- $K_{cx}\Delta_y$ by forcing the oscillation of the satellite around its Z axis through the thrusters the satellite,
- $(\eta_{cz}+\theta_{cz})$ by simultaneously forcing the oscillation of the satellite around its X axis and the test mass around its Z axis,
- $\left(\eta_{cy}-\theta_{cy}\right)$ by simultaneously forcing the oscillation of the satellite around its X axis and the test mass around its Y axis,
- K_{dx}/K_{cx} by forcing the oscillation of the satellite around its X axis,
- $\frac{\eta_{dz}+\theta_{dz}}{K_{cy}}$ by forcing the oscillation of the satellite around the T-SAGE Y axis,
- $\frac{\eta_{dy}-\theta_{dy}}{K_{cz}}$ by forcing the oscillation of the satellite around the T-SAGE Z axis,
- K_{2cxx}/K_{cx}^2 by forcing the oscillation of the satellite around the T-SAGE X axis,
- K_{2dxx}/K_{cx}^2 by forcing the oscillation of the satellite around the T-SAGE X axis.

The X axis is the axial direction of the test masses, maintained in the orbital plane. The EP test is performed along X. The Y and Z axes are the radial directions with Y being normal to the orbital plane during the test.

A standard duration of 10 orbits is selected for each calibration sequence. The sensors exhibit a differential noise spectral density of 2×10^{-12} $ms^{-2}/\sqrt{Hz}$ in high-resolution mode over the measurement bandwidth. The stimuli, either Earth's gradient, the oscillation of the satellite, or the forced motion of the test masses with respect to the satellite, generate an acceleration signal that is processed in the CMS to assess the parameters to be calibrated.

After one single round of calibration, data are reprocessed: each iteration improves the global accuracy as the assessment of all individual parameters benefits from the refinement of the other parameters that take part in the measurement equation. The accuracy required on the knowledge of the calibration parameters is reached after a few rounds.

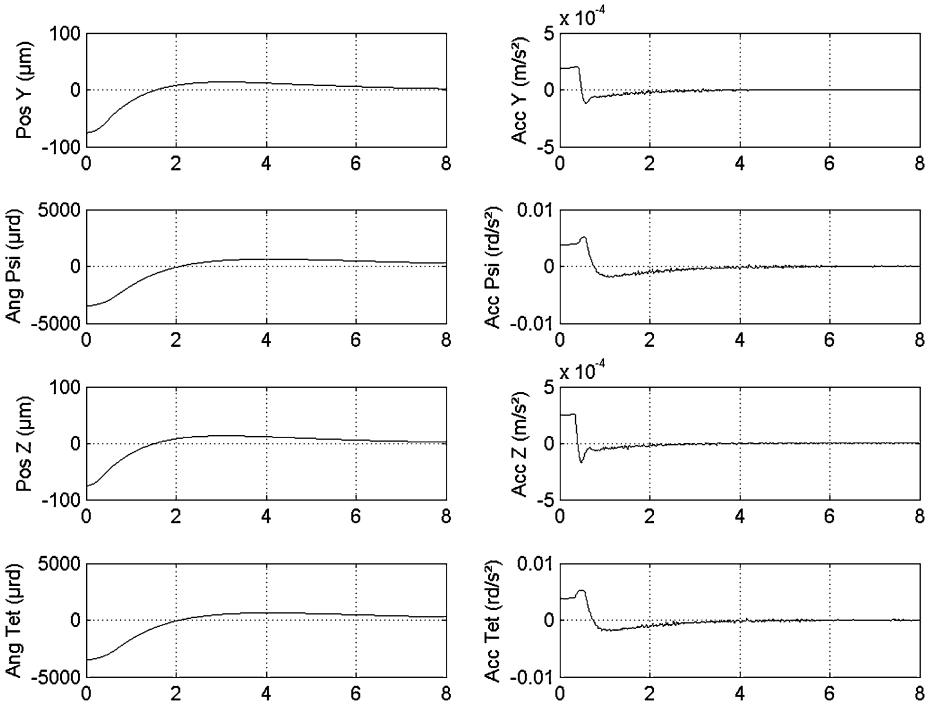

Fig. 5 Internal platinum test mass: simulation of levitation during a catapult test (8 seconds). The mass is swiftly controlled to the centre along the radial degrees of freedom Y, Z, Ψ and Θ. The front-end electronics is modified to boost the actuation and therefore reduce the levitation time

A full calibration campaign is scheduled every three months. The possible drift of the calibration parameters will be analysed and considered for the EP-test post-processing tasks. The correlation of this drift with the instrument temperature fluctuations will be particularly analysed.

3 On-ground Tests and Verification

The proof masses are too heavy for the electrostatic actuation delivered by the flight models to repel the 1g Earth's gravity acceleration. The final validation of the sensors is therefore conducted in a drop tower where 0-g conditions can be met, albeit during a brief time.

3.1 ZARM Drop-tower Test Campaigns

The ZARM drop tower offers three test configurations (Eigenbrod 2007):

– Standard drop lasting 4.7 seconds,
– Drop on-board a dedicated free-flyer capsule lasting approximately 4 seconds,
– Catapult shot extending the 0-g time to 9.3 seconds.

There is a trade-off between cleaner environment, lower vibrations and longer drop duration. The free-flyer capsule, located in a specific capsule, is released fractions of seconds after the

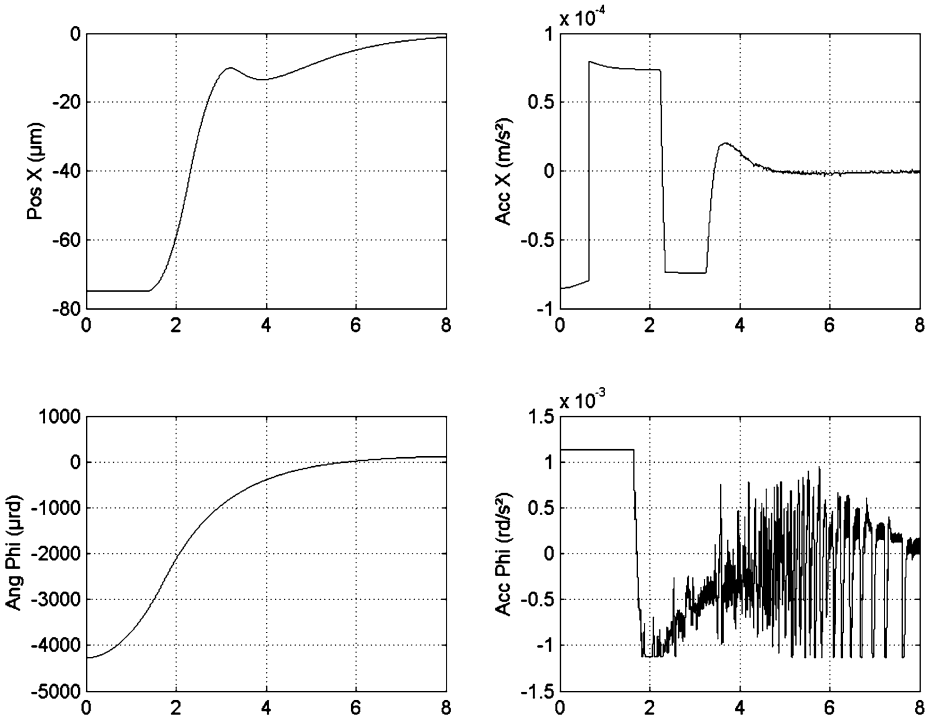

Fig. 6 Internal platinum test mass: simulation of levitation during a catapult test (8 seconds). Even with a scaled-up actuation range, on the EP axis, X, and the spin rotation around it, Φ, the feedback actuation is very weak, resulting in a very long transitional trajectory of levitation

drop and recaptured before final deceleration. In the meantime, approximately 4 seconds, it is flying freely inside the outer envelope. This set-up provides the free-flyer a cleaner gravitational trajectory, almost dragless. The free-flyer is also kept free of the vibrations originated in the response of the capsule structure and sub-systems to the release.

The electrostatic levitation of the T-SAGE test masses is limited by the inertia of the masses (approx. 1 kg each) in regard to the limited actuation provided by the electrostatic forces. Even with a modified front-end electronics dedicated to the tests, capable of delivering 90 volts to the electrodes, i.e., twice the flight-configuration maximum voltage, the validation of the levitation critically needs the extended time of 8 seconds offered by the catapult test as demonstrated in Fig. 5 for the radial axes and Fig. 6 for the EP axis and the spin axis.

3.2 Investigation on the Sensor Bias

The short duration of a drop-tower test makes it impossible to envisage calibration sequences like the one carried out in flight. Nonetheless, during a catapult test, the measurement of the acceleration along the drop axis coupled with the analysis of the capsule trajectory offers a practical way of assessing the sensor bias. The sensor biases are specified to be within $\pm 2.5 \times 10^{-8}$ m/s^2 along the EP axis X and within $\pm 5 \times 10^{-7}$ m/s^2 along the radial axes Y and Z.

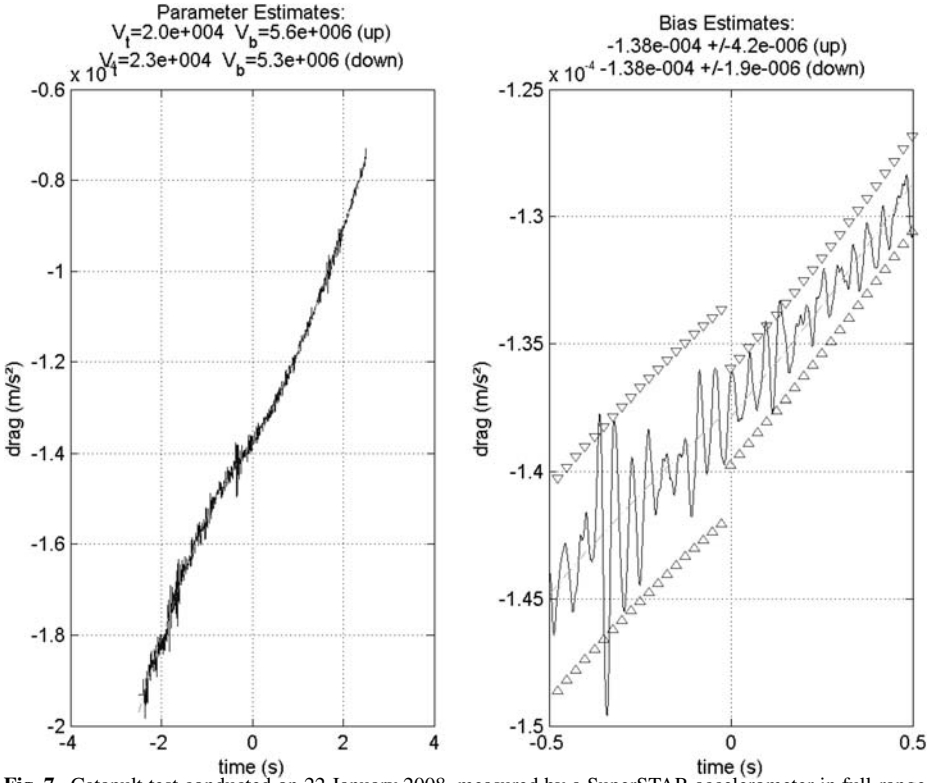

Fig. 7 Catapult test conducted on 22 January 2008, measured by a SuperSTAR accelerometer in full-range configuration along its X axis. The drag along the drop axis is captured and a model is fitted against the experimental data. The model parameters (V_t and V_d) are assessed on the *left graph*. The sensor bias is assessed from the model on the *right graph*: -1.3×10^{-4} m/s^2. The estimates from the descent offers a lower margin of error

In a standard drop, the drag due to the residual air pressure of less than 10 Pa in the tower is continuously increasing from the time of the capsule release to the end of the drop (Eigenbrod 2007). During a catapult shot the drag exerted on the capsule is null at the top of the trajectory, i.e., at the very precise moment when the velocity is also null. Being on-board the MICROSCOPE satellite, the accelerometers also senses the non-gravitational forces exerted on the instrument frame: drag and residual vibrations due to the structure response to the release. At the trajectory top, the drag is null and the vibrations due to the release are damped. The measurement picked up constitutes then an estimate of the sensor bias. A campaign has been conducted on a SuperSTAR accelerometer accommodated on the capsule used for the catapult tests. The SuperSTAR series of instrument was developed for the GRACE mission (Touboul 1999). It exhibits a resolution of $10^{-10}\,\mathrm{ms}^{-2}/\sqrt{\mathrm{Hz}}$ along its sensitive axes in high-performance configuration (Rodrigues et al. 2003).

The trajectory of the capsule is different whether the capsule is in its way up or down since the drag parameters are different on the ascent and the descent. Three contributors to the total surface force exerted on the capsule are considered:

– A "Stokes" term proportional to the velocity, $F_{\mathrm{Stokes}} = -\frac{g}{V_b}\dot{z}$,
– A "Rayleigh" term proportional to the square of the velocity, $F_{\mathrm{Rayleigh}} = -\frac{g}{V_t^2}\dot{z}$,
– A residual vibration force, $F_{\mathrm{vib}} = m_{\mathrm{cap}}\gamma_{\mathrm{vib}}$.

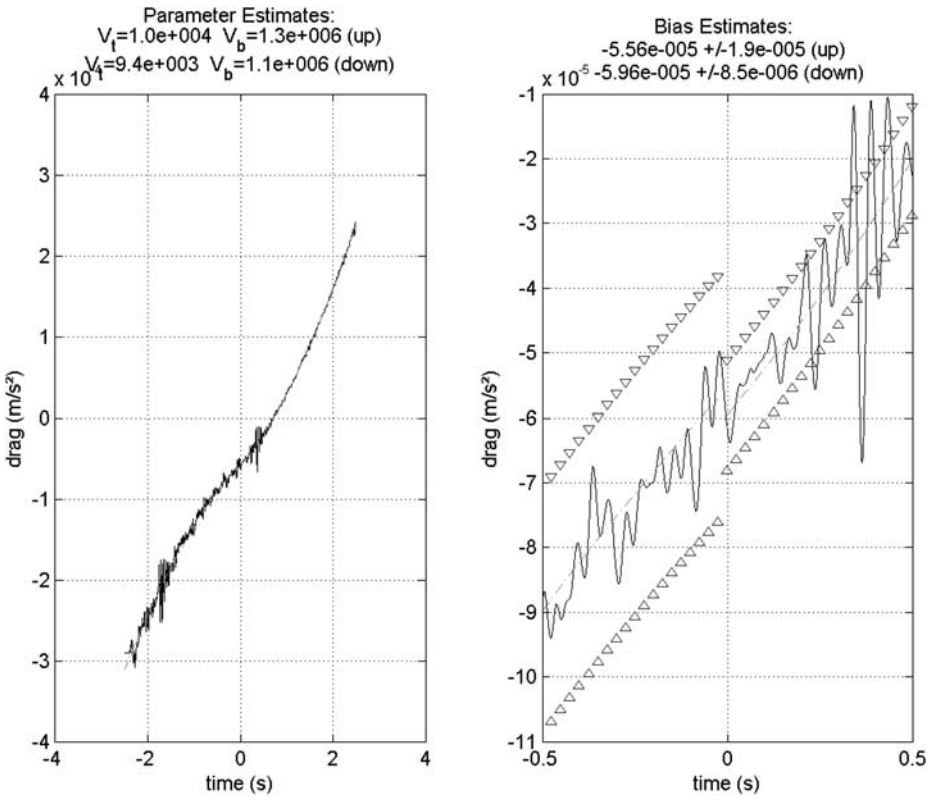

Fig. 8 Catapult test conducted on 15 February 2008, measured by a SuperSTAR accelerometer in high-performance configuration along its X axis. The drag along the drop axis is captured and a model is fitted against the experimental data. The model parameters (V_t and V_d) are assessed on the *left graph*. The sensor bias is assessed from the model on the *right graph*: -6×10^{-5} m/s^2. The estimates from the descent offers a lower margin of error

The capsule trajectory is described by the following equation:

$$m_{\text{cap}}\ddot{z} = -m_{\text{cap}}g + F_{\text{Stokes}} + F_{\text{Rayleigh}} + F_{\text{vib}}. \tag{9}$$

This is not a typical case of fluid physics: a lot of literature is available for either slow-speed bodies in viscous fluid or high-speed bodies in low-viscosity fluids but not for slow-speed bodies in low-pressure gas. As the scope of this article is to address a practical method to assess the sensor bias, the following analysis is focused on an accurate model of what the accelerometer senses rather than an analysis of the physics of the drop. The acceleration sensed by the accelerometer, γ_s, is modelled by a second-order polynomial:

$$\gamma_s|_{\text{up}} = -\frac{g^3}{V_{t_{\text{up}}}^2}(t - t_{\text{top}})^2 + \frac{g^2}{V_{b_{\text{up}}}}(t - t_{\text{top}}) + \gamma_{\text{vib}} + \gamma_n, \tag{10}$$

$$\gamma_s|_{\text{down}} = \frac{g^3}{V_{t_{\text{down}}}^2}(t - t_{\text{top}})^2 + \frac{g^2}{V_{b_{\text{down}}}}(t - t_{\text{top}}) + \gamma_{\text{vib}} + \gamma_n. \tag{11}$$

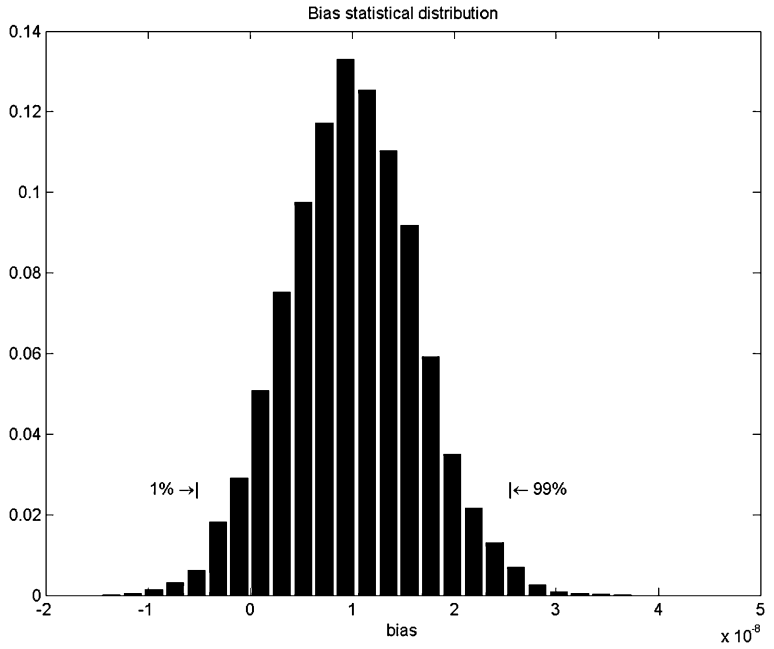

Fig. 9 Histogram of the biases computed on 3000 runs of simulation of a catapult test with fixed drag parameters and an additive noise originated in the measurement process with a standard deviation of 10^{-7} m/s^2. The 1st and 99th percentile are within $\pm\frac{6}{10}$ of its specified maximum value of $\pm 2.5 \times 10^{-8}$ m/s^2

Two conclusive catapult tests were conducted at the ZARM drop tower on 22 January 2008 and 15 February 2008. The first test was performed with the drag captured by the SuperSTAR accelerometer along its X axis in full-range mode, and the second in high-performance mode. The data are provided respectively in Fig. 7 and Fig. 8.

The SuperSTAR accelerometer bias assessed thanks to this is compatible with the performance analysis carried out on the instrument. One pattern has been clearly verified during this analysis: the bias is dependent on the mode of operation. The instrument performance analysis demonstrated that the accelerometer bias depends on the potential set onto the proof mass V_p to linearize the actuation: the higher the potential, the higher the bias. In full-range mode, it is 40 V and it is reduced to 10 V in high-performance mode. The ratio between full range and high performance is $1.3 \times 10^{-4}/6 \times 10^{-5} = 2.1$, thus verifying the performance analysis, albeit not to the level expected, i.e. 16.

3.3 Application on the MICROSCOPE On-ground Validation

The method presented in the previous paragraph is currently the only one that can result in a precise assessment of the T-SAGE sensor bias. One matter of concern is the sensitivity to the intrinsic noise of the sensor. The other contributors such as residual vibrations of the capsule have not been considered yet and thus are not factored in the following analysis. It will be investigated in the frame of the catapult tests.

A statistical analysis was conducted to evaluate the margin of error on the bias estimate due to the intrinsic noise of the sensor along the X axes. The standard deviation of the noise in full-range mode has been evaluated to 10^{-7} m/s^2. The bias assessment cannot be

conducted in the high-resolution configuration, because it takes too long a time for the mass to be properly levitated.

The histogram of Fig. 9 provides the distribution of the bias estimates for 10000 runs of simulated catapult tests. The drag parameters are constant (bias $= 10^{-8}$ m/s^2, $V_t = 1.5 \times 10^4$ m/s, $V_b = 6.5 \times 10^6$ m/s). For each run, a different normally distributed noise of standard deviation 10^{-7} m/s^2 is added to the drag measurement to simulate the accelerometer measurement. The model parameters are fitted against the runs of simulation and the bias is estimated. The distribution of the biases is normal with $3\sigma = \pm 1.4 \times 10^{-8}$ m/s^2.

The conclusion is that with the current performance, i.e., an accelerometer noise of standard deviation 10^{-7} m/s^2, the compliance of the sensor bias with the specification can be verified with a margin of error of $\pm 1.4 \times 10^{-8}$ m/s^2.

4 Conclusion

An overview of the challenging tasks of the on-ground and in-orbit calibration of the MICROSCOPE mission is provided in this article. A novel way of assessing the bias of the SAGE sensors is investigated.

Acknowledgements The authors wish to thank the MICROSCOPE mission teams at CNES, OCA and ZARM for the technical exchanges. This activity has received the financial support of CNES and ONERA.

References

C. Eigenbrod (The Drop Tower Operation and Service Company), *ZARM Drop Tower Bremen User Manual, 41* (ZARM FABmbh, Bremen, 2007)

É. Guiu, Étalonnage de la mission spatiale MICROSCOPE: optimisation des performances, 220. PhD Thesis, University of Nantes, 2007

M. Rodrigues, B. Foulon, F. Liorzou, P. Touboul, Flight experience on CHAMP and GRACE with ultra-sensitive accelerometers and return for LISA. Class. Quantum Gravity **20**, S291–S300 (2003)

P. Touboul, M. Rodrigues, The MICROSCOPE space mission. Class. Quantum Gravity **18**, 2487–2498 (2001)

P. Touboul, É. Willemenot, B. Foulon, V. Josselin, Accelerometers for CHAMP, GRACE and GOCE space missions: synergy and evolution. Boll. Geofis. Teorica Appl. **40**(3–4), 321–327 (1999)